WPPMI-CPR(18) 18938

F Subba et al.

Integrated Edge-Core Plasma Modelling for the EU-DEMO

Preprint of Paper to be submitted for publication in Proceeding of 23rd International Conference on Plasma Surface Interactions in Controlled Fusion Devices (PSI-23)

This work has been carried out within the framework of the EUROfusion Consortium and has received funding from the Euratom research and training programme 2014-2018 under grant agreement No 633053. The views and opinions expressed herein do not necessarily reflect those of the European Commission.

Integrated Edge-Core Plasma Modeling for the EU-DEMO

F. Subba[a,*], E. Fable[b], D. Coster[b]

[a] *NEMO Group, Dipartimento Energia, Politecnico di Torino, C.so Duca degli Abruzzi 24, 10129 Torino, Italy*
[b] *Max Planck Institut für Plasmaphysik, Boltzmannstraße 2, 85748 Garching bei Mnchen, Germany*

Abstract

We describe an integrated modeling of the EU-DEMO reactor, focusing on the possibility to obtain divertor-safe operations while keeping good fusion performances. This is done through a one-way coupling of the SOLPS and ASTRA codes, in which a produced edge plasma scenario provides proper boundary conditions for a core model, evaluating obtained fusion power and heating necessary to match separatrix conditions. It is found that, with assuming a constant Xe injection of $3 \times 10^{20}\ s^{-1}$, variable Ar concentrations can be used as a knot to produce target detachment through massive radiation, while keeping $P_{sep} > 150\ MW$, to guarantee H-mode operation. However, this requires an external heating value strongly increasing with the separatrix power, so that the net fusion produced drops to zero at $P_{sep} \sim 250\ MW$. This can limit the possibility to keep large P_{sep} values, which could be beneficial to facilitate He expulsion from the core. The narrow operational window observed is related to the fast growing Ar concentration in the external part of the pedestal needed to radiate the extra-power flowing out from the separatrix. Our simulations suggest an Ar concentration scaling as $c_{Ar} \propto P_{sep}^{5.8}$, surprisingly high if compared to other estimates available in the literature. Mechanisms which could contribute to explain such strong Ar dependence are proposed and qualitatively discussed.

Keywords: EU-DEMO, integrated modeling, SOLPS, ASTRA, High radiating

*Corresponding author

1. Introduction

The next proposed step after the ITER reactor along the path to the commercial exploitation of nuclear fusion reactions for energy production is the realization of a prototype demonstrative reactor, called DEMO. A number of designs are currently being considered in this respect [1, 2, 3], among which EURO-Fusion is focusing on the so-called European DEMO [3]. This should produce $\sim$ 2 (GW) of fusion power, out of which $\sim$ 150 (MW) are expected to cross the separatrix into the SOL, to robustly sustain H-mode operations [4]. Experimental scalings estimate the power radial decay length to be $\sim$ 1 (mm) at the OMP [5], while gyro-kinetic simulations [6] suggest that DEMO should operate in a regime not covered by current machines, resulting in a SOL width sensibly increased. However, even if the most optimistic predictions were correct, the surface available on the targets to accommodate for the power transported by the conduction/advection channel would hardly be of a few square meters. If we assume the usual power splitting between inner/outer divertor $\sim 0.3/0.7$, we easily estimate a power flux density on the targets of about 100 MW/m^2, far above current technological limits.

The most accepted solution to the overwhelming heat flux problem is to spread it over an area as large as possible by radiating it isotropically through injection in the SOL of carefully selected species. Previous discussion focused on Ar as a candidate impurity, mostly based on its high radiative efficiency at SOL characteristic temperatures [7]. However, this work analyzed only the divertor behavior, neglecting all possible feed-back on core performances. This analysis is not then capable to give conclusive informations, since any impurity present in the divertor region will also migrate in the core, where it will dilute the D-T fuel and eventually limit the available fusion power.

In this paper we extend the work described [7], with an analysis of the what the effect of Ar injected in the SOL could be on the core DEMO plasma. We do

this with a one-way coupling of the SOLPS and the ASTRA codes, where the 2D SOL transport code SOLPS is employed to produce a representation of the DEMO SOL plasma at various power and impurity injection levels. Information on the separatrix crossing power, species density and temperatures at the separatrix are then given to the 1D core transport ASTRA code, which is run to estimate the effect on the overall available fusion power.

The paper is structured as follows: in section 2 we briefly describe the numerical tools adopted, the coupling procedure and the expected uncertainties in the final result originating from the discrete approximation like, e.g., finite grid-size effects. In section 3 we discuss the main physical assumptions and approximations adopted. In section 4 we illustrate the results of our work, and finally in section we draw our conclusions, outlining possible implications for the reactor and open points which will deserve future investigation.

2. Numerical modeling

To model the SOL DEMO plasma we use SOLPS5.1 [8], a 2D toroidally symmetric multi-fluid code operating on a logically rectangular grid covering the inner part of the SOL, private flux region (PFR) and confined plasma. In the confined plasma region an artificial boundary is introduced ~ 10 cm inside the separatrix (at the OMP), to which proper boundary conditions have to be imposed. On the far SOL (and PFR) sides, the computational domain cannot extend up to the outer wall, and is truncated at an "artificial wall" boundary ~ 7 cm far in the SOL. The fluid transport equations are solved iteratively with a segregated approach closely following [9]. The various inner iteration levels are always solved up to an accuracy much higher than what is required to produce an accurate overall solution. Concerns sometimes arise with the outermost level, coincident with a transient time stepping, when un-complete convergence of the outermost loop may lead to failure in the global particle and energy conservation. However, this problem arises mostly when the code is run coupled with a Monte-Carlo module for neutral transport (se section 3), which

is not the present case. In all the cases described here, particle and energy conservation are fulfilled up to $\leq 10^{-3}$, which is expected not to produce noticeable results in the final solution. The computational grid is made by 96 (poloidal) $\times$ 46 (radial) cells. We did not estimate purposely the discretization error arising from this finite grid-size mesh, but we rely on a previous analysis reported in [10]. This was an analysis based on systematic mesh refinement, performed on cases not too different from the ones discussed in the following. It led us to estimate errors of the order of $\sim 20\%$ in the final results, which are values not larger the further uncertainties introduced by the physical model assumptions described below.

3. Physics model

The SOLPS physical model comprises the near SOL and PFRs. Although the grid extends into the core as previously described, the temperature at the core boundary is feedback-controlled in order to obtain the desired radial heat flux at the separatrix, so effectively reducing to the SOL the region physical interest. The particle balance is completed by a fuel source in the core region, effectively giving a separatrix particle flux of $\sim 7.7 \times 10^{21}\ s^{-1}$, and a D puff uniformly distributed along the outer wall boundary. The latter is changed during the simulation to feed-back control the electron separatrix density. Also impurities (Ar and Xe in our simulations) are introduced along the outer wall, at a constant rate (which was used as a scan parameter in our modeling). The pump effect is obtained at the PFR by allowing a neutral flux 3×10^{-3} times the sonic flux to leave the system, while at the targets full recycling is assumed (for particles) and 30% for the energy.

For all impurities (X_e and A_r) we adopt the bundled charge state model [11], reducing to three the effective number of different charged fluid computed per species. This gives a dramatic speed improvement, at the cost of some unaccuracy in the evaluation of the details of the radiative sources [12]. Neutrals

are modeled as an additional fluid species, as opposed to the alternative possibility: running the Monte Carlo transport model EIRENE, which would provide higher accuracy, especially in regions of low neutral density, at the cost of much higher CPU requirements. Both these approximations are expected to be eliminated in the future. Drifts are also not included, as common in many modeling at the current level of accuracy, based on the fact that drifts often slow down code convergence considerably. Following [7] we set radial transport coefficients in the SOL in order to obtain $\lambda_q \sim 3$ mm at the OMP. This is a value somehow in the middle of the range suggested by [5] and [6], and in line with previously published work. The actual coefficients experimentally selected to obtain the result are $D = 0.42$ and $\chi_e = \chi_i = 0.18\ m^2/s$. With this choice, the grid adopted places 4 cell centers within the first λ_q and 7 within the first $3\lambda_q$, where most of the interesting physics is expected to take place.

3.1. ASTRA modeling

Once the concentration of the seeded impurity(ies) is determined, this can be used as boundary condition for core simulation, which are performed with ASTRA [13]. This allows to estimate the performance, in terms of fusion and net power, of a scenario with that amount of seeding.

The scheme is the following: the core profiles of electron and ion temperature and of electron density are determined with some simplified transport model, such that a certain H factor (based on the ITER98(y,2) scaling) is reached (H = 1 in this case). The density profile is moderately peaked, with a peaking factor of ≈ 1.4. The pedestal top values are taken as 5.5 keV for the temperatures and 0.85 Greenwald fraction for the density.

Then, when the seeded impurity is present, auxiliary power is added in the core of the plasma sufficiently to make the separatrix power consistent with the SOLPS value to which a certain degree of seeding corresponds. This result in a self–consistent scenario in which the resulting net power (given by some thermal efficiency times fusion minus the auxiliary power) depends on the choice of the

separatrix power and the corresponding seeding level.

4. Results and discussion

We made scan on the separatrix crossing power P_{sep} to evaluate the Ar quantity in the plasma needed to drive detachment. In our modeling setup we introduce impurities by injecting them through the outer wall boundary. A natural way to measure the impurity presence would be then the imposed influx. However, much impurities influence radiation through its concentration, and often in the literature impurity presence is quantified through its concentration, defined as $c_z = n_z/n_e$, with n_z being the total density of a given impurity, including all charged states. In order to facilitate comparison with other models, we will adhere to the practice of using the concentration to measure the impurities presence. Except otherwise specified, A_r concentrations should always be intended as measured at the separatrix. As for X_e, we operated at a fixed puff level, corresponding to $3 \times 10^{20}\ s^{-1}$, which produced a relatively stable separatrix concentration level. The measured range varied between $c_{Xe} = 5.47 \times 10^{-5}$ and $c_{Xe} = 1.76 \times 10^{-4}$.

Figure 1 shows the effect of Ar concentration on outer target conditions. It is well known that DEMO should operate in detached divertor conditions. We prefer not to monitor detachment directly through the up/downstream pressure ratio; instead we look at target temperature and heat flux density, i.e. quantities directly related to the component lifetime. Figure 1 reports a line marking the conventional thresholds of 5 eV (left) or $10 MW/m^2$ (right). The first should guarantee that W sputtering is sufficiently low not to be a concern (in fact we neglect W in our simulations) [14], while the second is most often identified with the technological limit for tolerable steady-state heat fluxes [14]. In DEMO, achieving so low temperature and target heat flux can be done only if $\sim 90\%$ or more of P_{sep} can be radiated by impurities, which is compatible only with detached divertor conditions. In the following, we will conventionally call detached cases in which both the target temperature and heat flux density are

sufficiently low.

The figure reports scan done at different power levels, allowing to evaluate the impurity concentration needed to "detach", as a function of P_{sep}. The power split between ions and electrons is not uniform: at $P_{sep} = 150\ MW$, $45\ MW$ are given to electrons, and the remaining part to ions. The total power is varied by feeding only the ion channel, leading to very hot T_i upstream (a few KeV at the highest P_{sep} levels). This would correspond to a heating scheme giving energy selectively to ions, coupled with very long equipartition times. In DEMO, it is more likely that the actual power splitting will be less extreme. However, we thought interesting evaluating this condition as it represents a worst possible case from the radiation point of view, since radiation is effective at cooling the electrons as opposed to ions.

We observe that the dependence of target conditions on Ar concentration is not monotonic, noticeably for the level $P_{sep} = 180\ MW$. This is not impossible, since the Ar radiation efficiency is a strongly non-linear and non-monotonic function of the electron temperature, opening the possibility to obtain the same radiation level at different global plasma conditions. There is no obvious reason why such possibility should be limited to a single (or narrow range of) P_{sep} level. More likely, the possibility to observe this bifurcated behavior would depend in experiments on the transient evolution leading to a given steady-state. In the modeling this question should be addressed by detailed time-dependent simulations performed with carefully selected initial conditions. This aspect was not considered in our study, and will be addressed in a future work.

Combined analysis both parts of figure 1 allows determining, for each power level, the minimum Ar concentration required to obtain "detached" conditions. Results are reported in figure 2. For each power level considered, the reported triangle marks the last computed non-detached point, and the circle is the first detached one. The dashed line is the least-square-error approximation of the mid-values between circles and triangles. The strikingly surprising point is that a very good representation for this line is $c_{Ar} \propto P_{sep}^{5.8}$, a huge value if compared with the traditional scaling $c_{Ar} \propto P_{sep}$ [15].

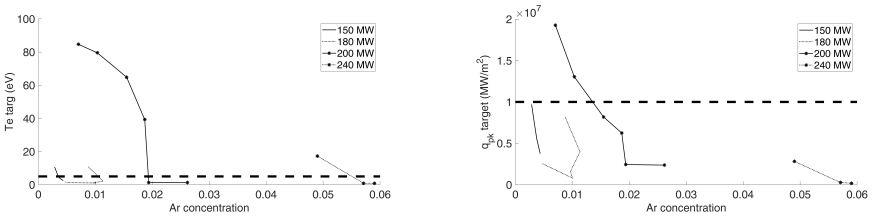

Figure 1: Effect of the separatrix Ar concentration on target conditions. Left: max. target electron temperature vs. Ar concentration. Right: max target heat flux density vs. Ar concentration.

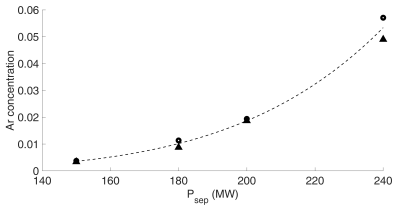

Figure 2: Ar concentration level required to obtain detachment as a function of P_{sep}. Triangles: lower limit. Circles: upper limit. The dashed interpolating line is close to $c_{Ar} \propto P_{sep}^{5.8}$

The mechanism why the impurity at the separatrix needed to detach is larger than expected may be related to different reasons. Part of this can be related to our choice to heat preferentially ions, so that power must be first transferred to electrons and then radiated, as opposed to [15] which assumes equal power split. Another contribution can arise from the importance of far-SOL processes, i.e. radial transport. This is explained in figure 3. This shows the Ar concentration along the tube (taken from the X point down to the outer target) as a function of the Ar concentration just inside the separatrix for two flux tubes close to the separatrix and about 11 mm (i.e. more than 3 λ_q) deep in the SOL (measured at the OMP), and the power radiated along the two same flux tubes (identified here with the width of a mesh radial cell). The picture makes it clear (left) that the Ar concentration inside the separatrix is not strongly correlated to the Ar concentration along the different flux tubes, especially for the outer flux tubes. In particular, the Ar concentration along the flux tubes initially increases with the concentration inside the separatrix, but at some point

presents a sharp drop. This is related to the neutrals penetration depth, which increases when the separatrix temperature drop. Below some T_e threshold, Ar atoms enter preferentially the confined plasma before being ionized (probably also because in our setup Ar is puffed all along the outermost flux surface) with respect to the atoms stopped in the SOL. On the other hand, figure 3 right shows that the outermost flux tubes are critical to detach the target (we check our detachment conditions all along the target), since they reach that condition later. Detachment, at least according to the present definition, will then be obtained only when the Ar concentration *in the far SOL* becomes sufficiently large, which might require extremely large concentrations *inside the separatrix*.

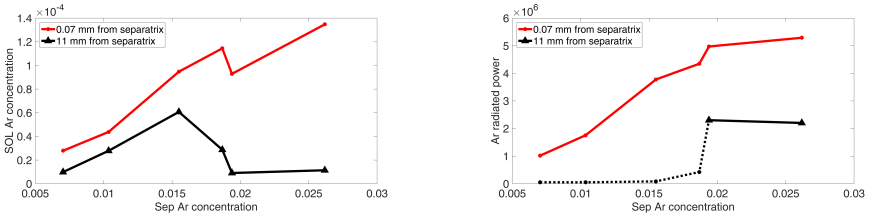

Figure 3: Left: Ar concentration along two flux tubes as a function of the concentration inside the separatrix. Right: Power radiated along two flux tubes as a function of the Ar concentration inside the separatrix. Solid lines correspond to detached conditions, dotted line to attached plasma.

As an additional warning, we should stress that the results depends sensitively on the actual transport law chosen. To test this, we repeated a number of cases by multiplying/dividing either D or $\chi_{e,i}$ by a factor 1.5, and tested the sensitivity of the peak target temperature $T_{e,pk}$ and the peak heat flux density on target q_{pk} on D or $\chi_{e,i}$. The temperature sensitivity on D was defined as $S_{T,D} = \left|\frac{\Delta T}{T} \cdot \frac{D}{\Delta D}\right|$, and similarly for the other considered dependencies. The average values we found are: $S_{T,D} = 2.8$, $S_{T,\chi} = 1.1$, $S_{q,D} = 2.0$, $S_{q,\chi} = 0.8$. Although these values are not surprising in absolute values (figure 2 clearly show that the problem is particularly sensitive to input conditions, especially close to detachment), they classify the choice of transport as a serious uncertainty

P_{sep} MW	P_{net} MW
150	450
180	370
190	280
200	160
250	< 0

Table 1: Net electrical power P_{net} as a function of the assigned separatrix power P_{sep}. The values are rounded to the first position.

source in our model.

4.1. ASTRA physics results

The physics results of the modeling performed in ASTRA are obtained following variations on the assumption of the transport of the seeded impurity in the plasma. In principle the most optimistic case is when the pedestal screens the impurity, producing a hollow pedestal profile [16].

In the present work, an assumption of flat density is assumed, that is, the seeded impurity has the same density throughout the whole plasma region, with the value given by the separatrix density obtained in the SOLPS simulations. This assumption is probably the safest considering that edge transport, may it be ELMy, harmonic oscillations, or weakly coherent mode in I–mode, it will basically flatten out the edge profile of a source–free species [17]. For the core part (i.e. from pedestal top to magnetic axis) one expects roughly flat density since neoclassical transport is small and turbulence transport for high–Z impurities gives flat profiles [18].

Given the flat density assumptions, the result for the fusion power and for the net power (defined as $P_{\mathrm{net}} = 0.35(P_{\mathrm{fus}} + P_{\mathrm{aux}}) - P_{\mathrm{aux}}/0.4$) are given in the table 1. The results presented in the table show that, with the seeding defined by SOLPS results, the optimal net power sits at the minimum P_{sep}, that is, there is no gain in increasing the heating in the plasma if the losses are dominated

by the seeding impurity, which concentration scales as much as $P_{\rm sep}^{5.8}$. This is in contrast to a situation in which the seeded impurity does not dominate the losses, in which instead it is beneficial to increase the separatrix power, since it allows both larger profile gradients and at the same time, due to the increased transport, facilitates the expulsion of He.

5. Conclusions

In this paper we presented a first integrated study of the influence of impurities on DEMO in terms of both, target conditions and fusion performance. Our simulations suggest that it is possible to reach target detached conditions with an amount of impurity which is still compatible with acceptable core performances. However, at least for the setup we focused on in this study, the core impurity concentration grows up very quickly with the separatrix-crossing power. This results in fast degradation of fusion performance when additional heating is added to the plasma, so that the optimum condition seems to be obtained when no additional heating at all is considered. This, in turn, may have drawbacks as, for example, a more difficult He exhaust, which is however not considered in this paper.

The observed strong dependence of separatrix impurity concentration on P_{sep} is not consistent with previous proposed scalings. We tried to point-out some mechanisms which could potentially explain this difference. A further dedicated study aiming at confirming and explaining in more detail this finding is under way.

Acknowledgements

This work has been carried out within the framework of the EUROfusion Consortium and has received funding from the Euratom research and training programme 2014-2018 under grant agreement No 633053. The views and opinions expressed herein do not necessarily reflect those of the European Commission.

References

[1] K. Tobita, N. Asakura, R. Hiwatari, Y. Someya, H. Utoh, K. Katayama, A. Nishimura, Y. Sakamoto, Y. Homma, H. Kudo, Y. Miyoshi, M. Nakamura, S. Tokunaga, A. A. and, Design strategy and recent design activity on japan's DEMO, Fusion Science and Technology (2017) 1–9.

[2] Y. Wan, J. Li, Y. Liu, X. Wang, V. Chan, C. Chen, X. Duan, P. Fu, X. Gao, K. Feng, S. Liu, Y. Song, P. Weng, B. Wan, F. Wan, H. Wang, S. Wu, M. Ye, Q. Yang, G. Zheng, G. Zhuang, Q. L. and, Overview of the present progress and activities on the CFETR, Nuclear Fusion 57 (10) (2017) 102009.

[3] G. Federici, C. Bachmann, W. Biel, L. Boccaccini, F. Cismondi, S. Ciattaglia, M. Coleman, C. Day, E. Diegele, T. Franke, M. Grattarola, H. Hurzlmeier, A. Ibarra, A. Loving, F. Maviglia, B. Meszaros, C. Morlock, M. Rieth, M. Shannon, N. Taylor, M. Tran, J. You, R. Wenninger, L. Zani, Overview of the design approach and prioritization of r&d activities towards an EU DEMO, Fusion Engineering and Design 109-111 (2016) 1464–1474.

[4] Y. R. Martin, T. Takizuka, the ITPA CDBM H-mode Threshold Data Group, J. Phys.: Conf. Ser. 123 (2008) 012033.

[5] T. Eich, A. Herrmann, G. Pautasso, P. Andrew, N. Asakura, J. Boedo, Y. Corre, M. Fernstermacher, C. Fuchs, W. Fundamenski, G. Federici, E. Gauthier, B. Goncalves, O. Gruber, A. Kirk, A. Leonard, A. Loarte, G. Matthews, J. Neuhauser, R. Pitts, V. Riccardo, C. Silva, Power deposition onto plasma facing components in poloidal divertor tokamaks during type-i elms and disruptions, Journal of Nuclear Materials 337-339 (2005) 669–676.

[6] C. Chang, S. Ku, A. Loarte, V. Parail, F. Kchl, M. Romanelli, R. Maingi, J.-W. Ahn, T. Gray, J. Hughes, B. LaBombard, T. Leonard, M. Makowski,

J. Terry, Gyrokinetic projection of the divertor heat-flux width from present tokamaks to ITER, Nuclear Fusion 57 (11) (2017) 116023.

[7] F. Subba, L. Aho-Mantila, D. Coster, G. Maddaluno, G. F. Nallo, B. Sieglin, R. Wenninger, R. Zanino, Modelling of mitigation of the power divertor loading for the EU DEMO through ar injection, Plasma Physics and Controlled Fusion 60 (3) (2018) 035013.

[8] R. Schneider, X. Bonnin, K. Borrass, D. Coster, H. Kastelewicz, D. Reiter, V. Rozhansky, B. Braams, Plasma edge physics with b2-eirene, Contributions to Plasma Physics 46 (1-2) (2006) 3 – 191.

[9] S. V. PATANKAR, Numerical Heat Transfer and Fluid Flow, Hemisphere, Washington, D.C., 1980.

[10] F. Subba, Final report on deliverable solps simulations of plasmas in demo (2017).
`https://idm.euro-fusion.org/?uid=2MR5BN&action=get_document`

[11] X. Bonnin, D. Coster, Full-tungsten plasma edge simulations with SOLPS, Journal of Nuclear Materials 415 (1) (2011) S488–S491.

[12] D. P. Coster, Reduced physics models in SOLPS for reactor scoping studies, Contributions to Plasma Physics `doi:10.1002/ctpp.201610035`.

[13] E. Fable, C. Angioni, F. J. Casson, D. Told, A. A. Ivanov, F. Jenko, R. M. McDermott, S. Y. Medvedev, G. V. Pereverzev, F. Ryter, W. Treutterer, E. V. and, Novel free-boundary equilibrium and transport solver with theory-based models and its validation against ASDEX upgrade current ramp scenarios, Plasma Physics and Controlled Fusion 55 (12) (2013) 124028.

[14] R. Wenninger, M. Bernert, T. Eich, E. Fable, G. Federici, A. Kallenbach, A. Loarte, C. Lowry, D. McDonald, R. Neu, T. Ptterich, P. Schneider,

B. Sieglin, G. Strohmayer, F. Reimold, M. Wischmeier, DEMO divertor limitations during and in between ELMs, Nucl. Fusion 54 (11) (2014) 114003.

[15] R. Goldston, Heuristic drift-based model of the power scrape-off width in low-gas-puff h-mode tokamaks, Nuclear Fusion 52 (1) (2011) 013009.

[16] R. Dux, A. Loarte, C. Angioni, D. Coster, E. Fable, A. Kallenbach, The interplay of controlling the power exhaust and the tungsten content in ITER, Nuclear Materials and Energy 12 (2017) 28–35.

[17] A. Polevoi, A. Loarte, R. Dux, T. Eich, E. Fable, D. Coster, S. Maruyama, S. Medvedev, F. Kchl, V. Zhogolev, Integrated simulations of h-mode operation in ITER including core fuelling, divertor detachment and ELM control, Nuclear Fusion 58 (5) (2018) 056020.

[18] C. Angioni, R. Bilato, F. Casson, E. Fable, P. Mantica, T. Odstrcil, M. Valisa, and, Gyrokinetic study of turbulent convection of heavy impurities in tokamak plasmas at comparable ion and electron heat fluxes, Nuclear Fusion 57 (2) (2016) 022009.